‚Supplementary File

Fall and Rise: Disentangling Cycle Life Trends in Atmospheric Plasma-Synthesized FeOOH/PANI Composite for Conversion Anodes in Lithium-Ion Batteries

Evgenii V. Beletskii *[1], Alexey I. Volkov [1], Ksenia A. Kharisova [1], Oleg V. Glumov [2], Maksim A. Kamarou [3], Daniil A. Lukyanov [1] and Oleg V. Levin *[1]

[1] Institute of Chemistry, St. Petersburg State University, St. Petersburg, Universitetskaya Emb.7/9, 199034, Russian Federation; a.i.volkov@spbu.ru (A.I.V.); st111412@student.spbu.ru (K.A.K.); lda93@yandex.ru (D.A.L.)
[2] Research Park, St. Petersburg State University, St. Petersburg, Universitetskaya Emb.7/9, 199034, Russian Federation; o.glumov@spbu.ru
[3] Belarusian State Technological University, 220006 Minsk, Republic of Belarus; makkom1995@gmail.com
* Correspondence: e.beletsky@spbu.ru (E.V.B.); o.levin@spbu.ru (O.V.L.); Tel. +7-(812)-3636000, Ext. 9801

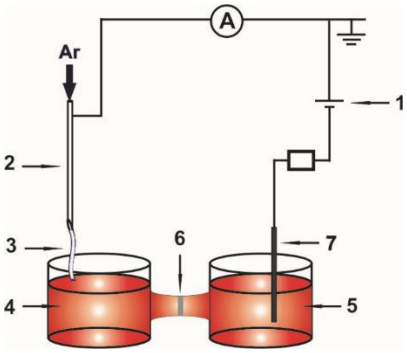

1 – DC power supply, 2 – a stainless steel capillary tube anode, 3 – plasma discharge, 4 – anolyte, 5 – catholyte, 6 – a glass microfiber filter, 7 – stainless steel mesh cathode

Figure S1. Synthesis setup diagram

XPS measurements were conducted with photoelectron spectrometer Thermo Fisher Scientific Escalab 250Xi with AlKα radiation (photon energy 1486.6 eV). Spectra were recorded in the constant pass energy mode at 50 eV for element core level spectrum and 100 eV for survey, using XPS 650 μm spot size with total energy of 0.2 eV. To counter the surface charge caused by emitting photoelectrons dual mode charge compensation (a combination of low energy electrons and argon) was used. Investigations were conducted at room temperature in an ultrahigh vacuum of the order of 10^{-9} mbar. Peaks were fitted with a product of asymmetric Gaussian and Lorentzian lineshape.

XRD powder X-ray diffraction (Bruker D2 Phaser with the following conditions: CoKα1+2 radiation with 30 kV/10 mA, $\lambda_{CoK\alpha1}$ = 1.78897 Å and $\lambda_{CoK\alpha2}$ = 1.79285 Å, the position sensitive detector, the Bragg-Brentano parafocusing geometry, rotation speed = 20 rpm, range of diffraction angles 2θ=(5–75)° with a step size of 0.02°, point exposure = 0.5 s, air, T = 25 °C).

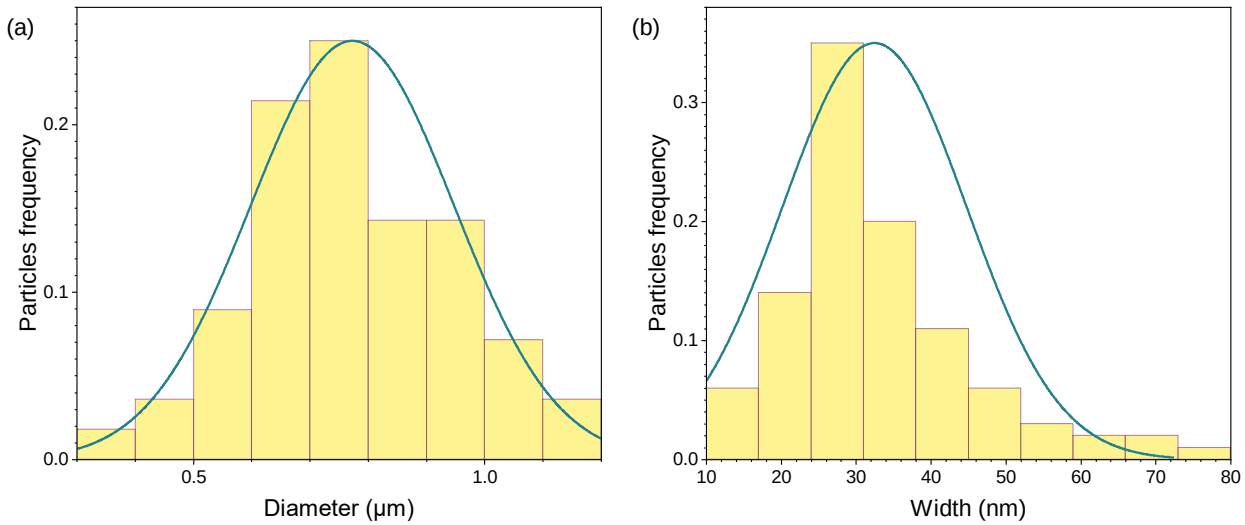

Figure S2. FeOOH/PANI powder particles sizes distribution estimated from SEM images: diameter of urchin-like spheres (a) and width/thickness of needles (b).

The XRD pattern of the synthesized material is shown in Figure S3. The diffractogram does not contain any peaks related to PANI due to the high amorphous nature of the material. Nevertheless, the diffraction peaks correspond to those of schwertmannite (PDF 47-1775), including the peaks at 20.17°, 30.49°, 33.54°, 41.18° and 52.44°. The shift of the peaks with respect to the reference is caused by the different material of the X-ray tube anode and the different X-ray lengths (1.5406 Å for copper vs 1.7902 Å for cobalt).

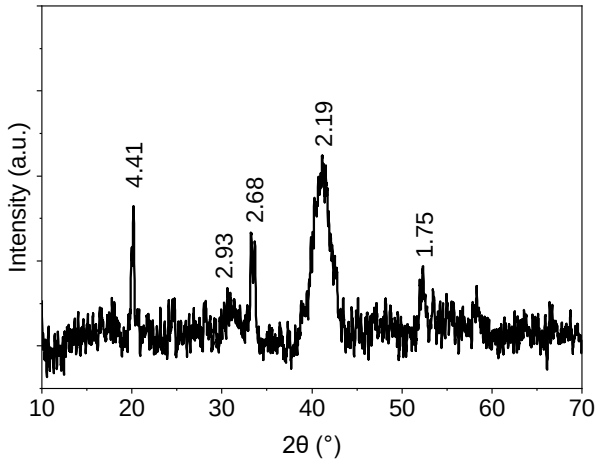

Figure S3. XRD of FeOOH/PANI particles labeled with d-spacing (Å) values.

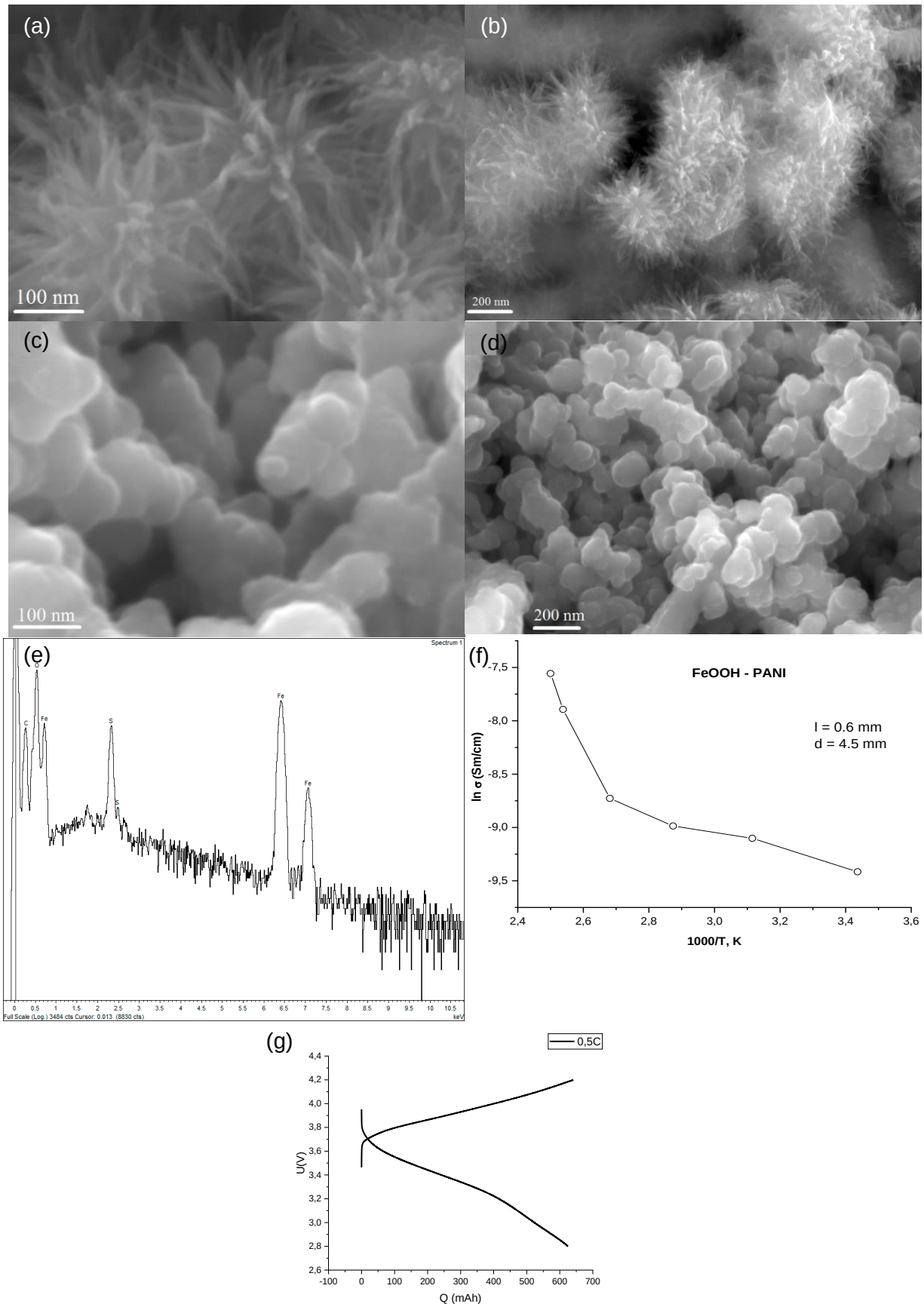

Figure S4. SEM images of plasma solution synthesized FeOOH (a, b) and PANI (c,d) nanoparticles; EDX spectra of FeOOH/PANI composite (e); electrical conductivity temperature dependence of FeOOH/PANI composite (f); charge-discharge curve of the NMC532 - Graphite full cell at a C/2 rate (g).

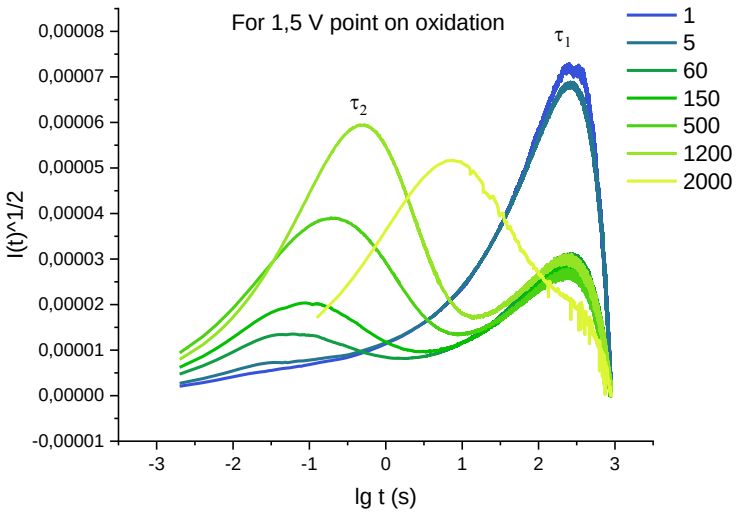

Figure S5. Cottrell function plot for the current transient versus the decimal logarithm of time

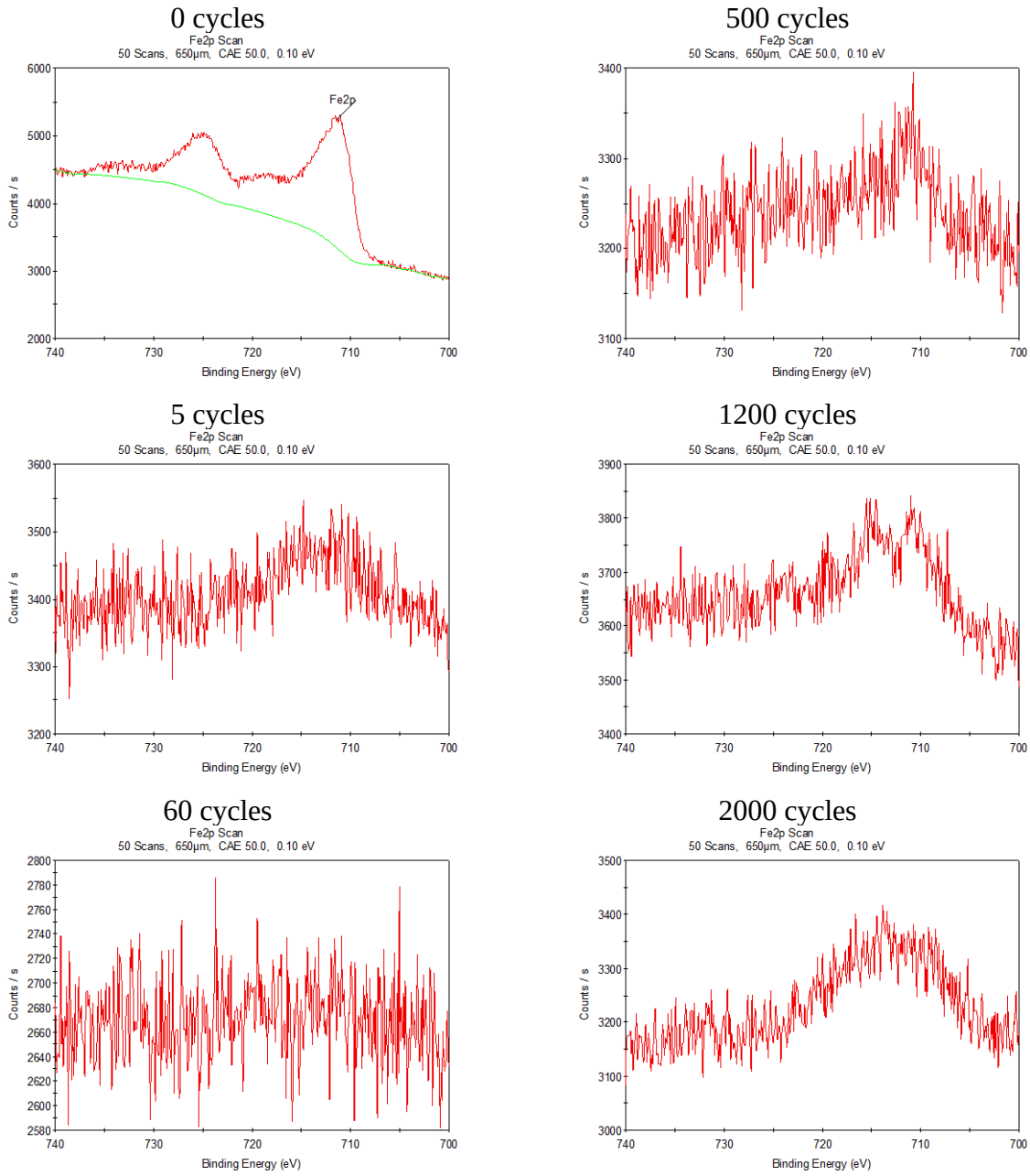

Figure S6. XPS spectra of Fe 2p

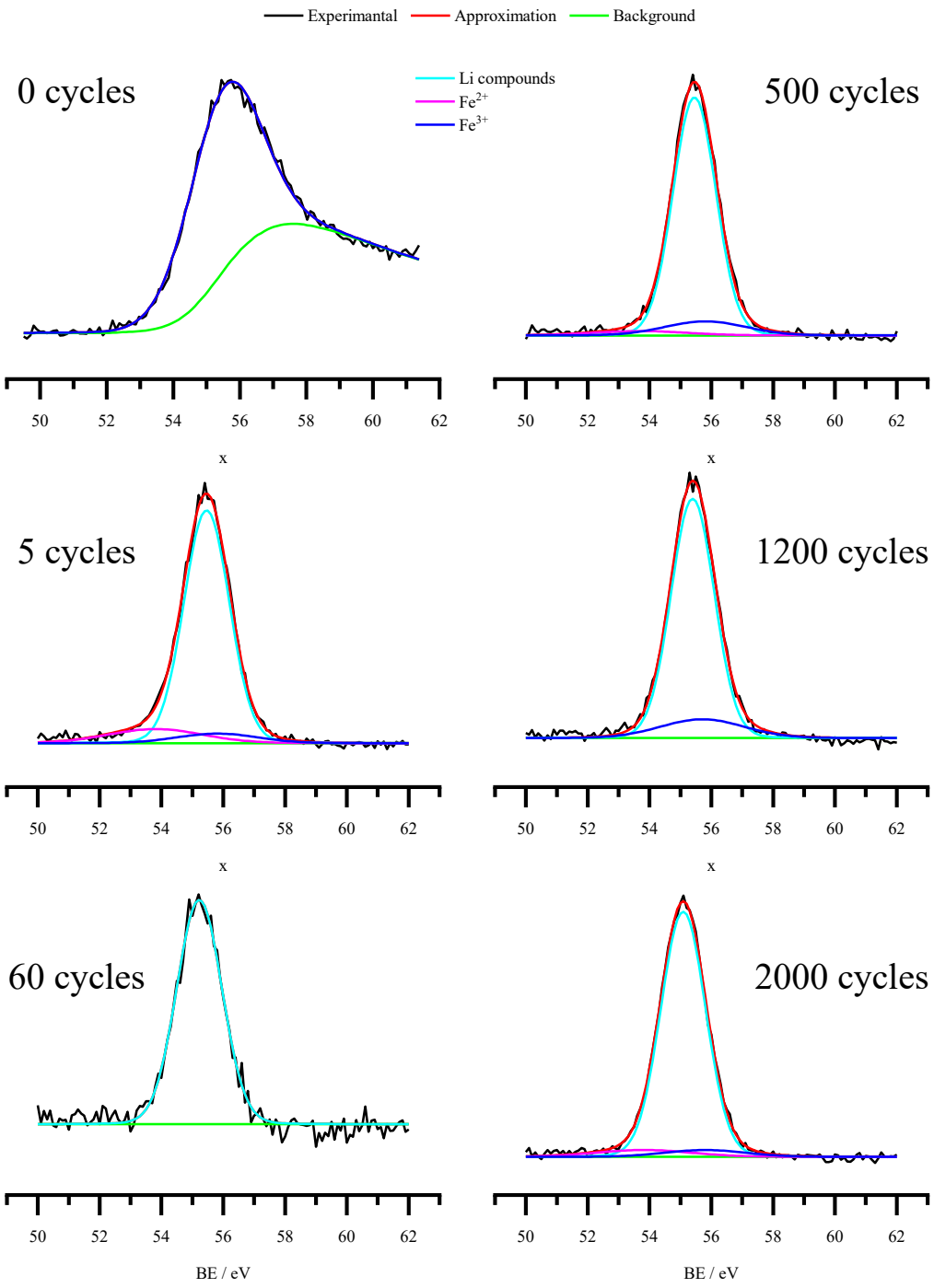

Figure S7. XPS spectra of Li 1s + Fe 3p

0	5	60	500	1200	2000

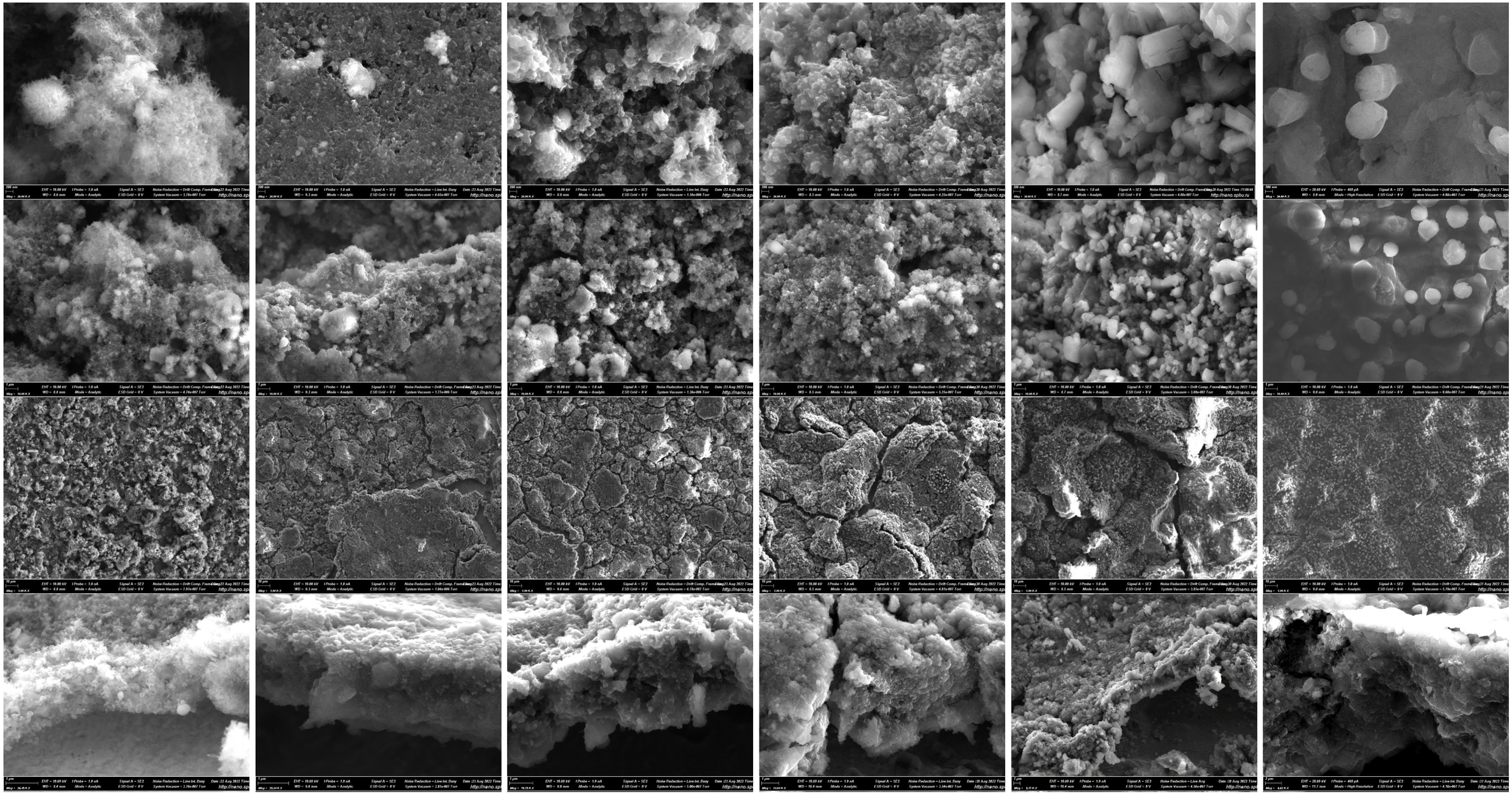

Figure S8. Evolution of the electrode surface during 2000 cycles